Ore Geology Reviews 66 (2015) 334–343

Contents lists available at ScienceDirect

Ore Geology Reviews

journal homepage: www.elsevier.com/locate/oregeorev

Origin and age of rift related fluorite and manganese deposits from the San Rafael Massif, Argentina

Nora A. Rubinstein [a,*], Eduardo O. Zappettini [b]

[a] Instituto de Geociencias Básicas, Aplicadas y Ambientales (IGEBA, UBA-CONICET) Departamento de Ciencias Geológicas, Pabellón II, Ciudad Universitaria, C1428EHA, Buenos Aires, Argentina
[b] Instituto de Geología y Recursos Minerales, Servicio Geológico Minero Argentino, Avda, General Paz 5445, Edificio 25, B1650KNA Buenos Aires, Argentina

ARTICLE INFO

Article history:
Received 4 July 2014
Received in revised form 23 October 2014
Accepted 6 November 2014
Available online 13 November 2014

Keywords:
Isotopes and geochemistry
Fluorite and manganese
Detachment related deposits
San Rafael Massif
Argentina

ABSTRACT

The San Rafael Massif is characterized by widespread fluorite and manganese epithermal ore deposits whose origin has been under debate to the present. Isotopic (Sm/Nd and K/Ar) and geochemical (trace elements and REE) data of fluorite and manganese ore allowed to establish the age and genesis of the deposits and to propose a regional genetic model. The fluorite deposits were formed during the Upper Triassic–Lower Jurassic as a result of the Triassic rifting that launched a hydrothermal activity at regional scale. The hydrothermal fluids had low T and high fO_2 with fluorine probably derived from a mantle source and REE scavenged from the volcanics of the Gondwanan Choiyoi Magmatic Cycle upper section. The manganese deposits were formed by oxidizing hydrothermal fluids that collected Mn from deep sources and also leached REE from the upper section of the Choiyoi Magmatic Cycle during two mineralization episodes. One episode was linked to the rift tectonic setting that remained active up to the Upper Cretaceous and the other was related to an Early Miocene back-arc extensional geodynamic setting. Both manganese and fluorite deposits were formed in extensional tectonic settings within an epithermal environment near the surface, and can be ascribed to the general model of detachment-related deposits.

1. Introduction

The San Rafael Massif (SRM), located in south-central part of the province of Mendoza, Argentina (Fig. 1), is characterized by widespread volcanic and pyroclastic rocks of Gondwanan age, known as the Choiyoi Magmatic Cycle (CMC). Two different sections can be distinguished within this volcanic sequence.The lower section (Early to Middle Permian) was emplaced syntectonically with the San Rafael Orogeny (SRO) (Kleiman and Japas, 2009) and has geochemical features that indicate a magmatic arc setting (Llambías et al., 1993; Kleiman and Japas, 2009 and references therein). The upper section (Middle to Late Permian) was emplaced during the Post-San Rafael extension (PSRO) (Kleiman and Japas, 2009) and shows geochemical characteristics transitional between subduction and continental intraplate settings (Llambías et al., 1993; Kleiman and Japas, 2009 and references therein).

Based on stratigraphic and isotopic constraints the main ore deposits in the SRM have been linked to the CMC (Carpio et al., 2001; Rubinstein et al., 2004). Several Cu–(Mo) porphyry type deposits are hosted and genetically linked with the lower section of the CMC (Delpino et al., 1993; Rubinstein et al., 2012; Gómez and Rubinstein, 2010a, 2010b). Genetically related to the upper section of the CMC there are Mo-porphyry type deposits (Carpio et al., 2001) and epithermal low-sulfidation deposits (Rubinstein and Gargiulo, 2005; Gargiulo et al., 2007). The different mineralization styles in the upper and lower sections of the CMC were linked to the evolution of the Permian magmatic arc under a changing tectonic regime (Carpio et al., 2001). Fluorite and manganese vein systems, mainly hosted by rocks of the upper section, are regionally distributed. The origin of the fluorite and manganese deposits and the link between them is up to date controversial (eg. Mallimacci et al., 2010 and references therein).

The aim of this paper is to present the first isotopic and geochemical data of fluorite and manganese ore deposits of the SRM, which contribute to reveal their ages and genesis, allowing establishing a single regional metallogenic model for both mineralizations.

2. Geological setting

The geology of the southern part of the SRM, where most fluorite and manganese deposits are concentrated, is shown in Fig. 1. The oldest rocks include high grade metamorphic rocks, granites, aplites and pegmatites of Grenvillian age (Cingolani and Varela, 1999). During the Early Palaeozoic, carbonatic and clastic sediments were deposited and metamorphosed by the Famatinian Orogeny (Criado Roque, 1972; Bordonaro et al., 1996). This was followed by Carboniferous–Lower Permian glacimarine and continental sedimentation folded during the SRO (González Díaz, 1972; Espejo and López Gamundi, 1994 among others).

* Corresponding author. Tel./fax: +54 114576 3300 phone internal 313.
E-mail address: nora@gl.fcen.uba.ar (N.A. Rubinstein).

http://dx.doi.org/10.1016/j.oregeorev.2014.11.004
0169-1368/

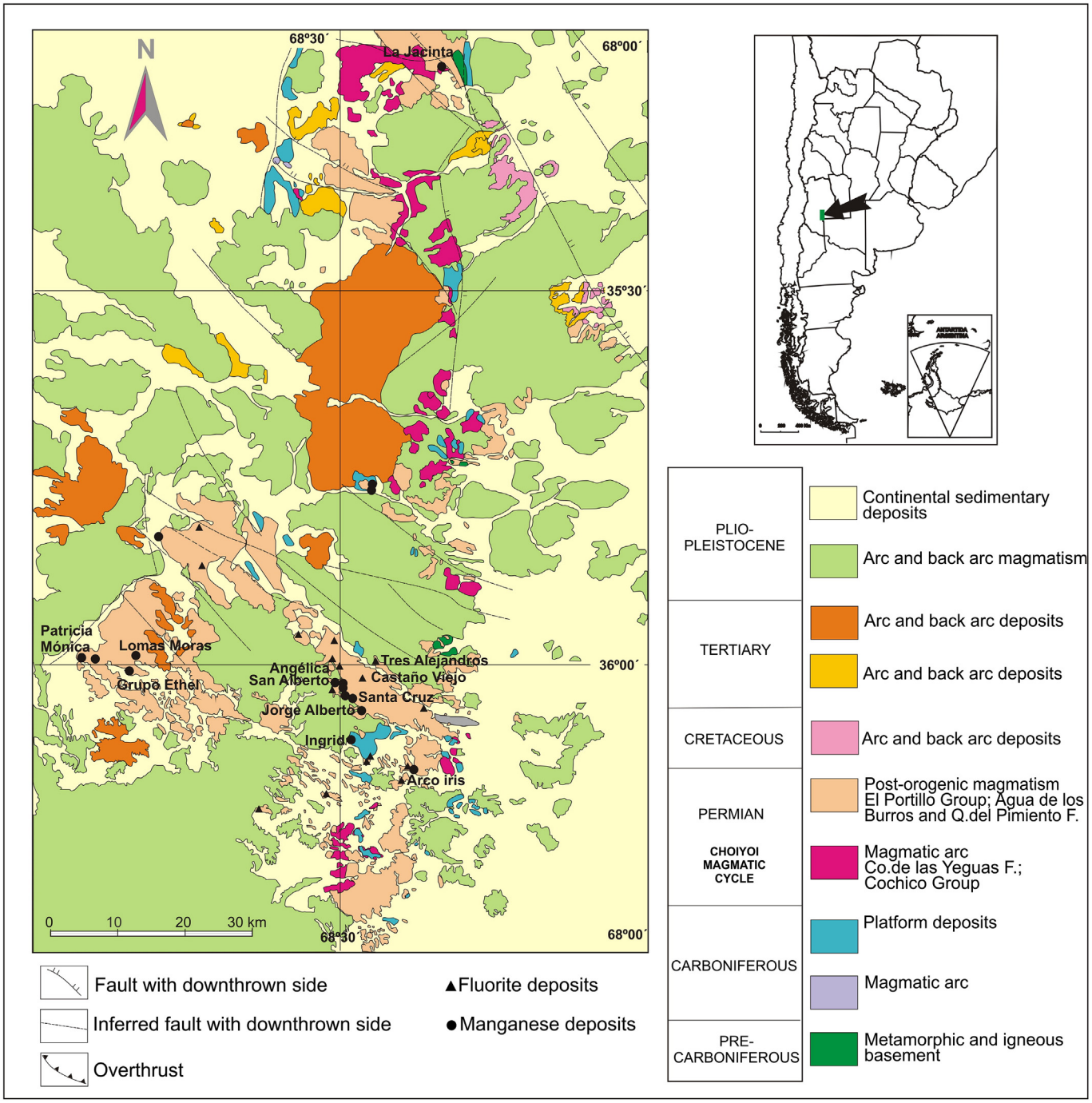

Fig. 1. Geology of the southern part of the SRM with the location of the main fluorite and manganese ore deposits including those that were studied for this paper (modified from Carpio et al., 2001).

During the Late Paleozoic there was an active arc on the western proto-margin of Gondwana that produced the CMC which was followed by Middle Triassic synrift-continental successions which are interbedded with slightly alkaline rhyolites, ignimbrites and basalts (Kleiman and Salvarredi, 2001). The emplacement of the Triassic rocks was controlled by NW tensional, WNW and NNW transtensional faults, which also continued deforming the Triassic rocks (Japas et al., 2005).

From the Late Cretaceous to the Pliocene, the geological record shows sequences of continental sedimentary rocks and volcanic-arc and back-arc products, including pyroclastic and siliceous to basaltic volcanic rocks, which were deformed during different phases of the Andean Orogeny. Back-arc basaltic volcanism and sedimentation continued from the Pliocene to the Pleistocene (Sepúlveda et al., 2007a, 2007b).

2.1. The Choiyoi Magmatic Cycle

The CMC extends along the western protomargin of Gondwana between 28° and 42°S in Argentina and Chile (Llambías et al., 1993). Particularly in the SRM two different sections can be distinguished within this volcanic sequence (Llambías et al., 1993). The lower section (281.4 ± 2.5 up to 264.8 ± 2.3 Ma, Rocha-Campos et al., 2011) consists mainly of andesites and dacitic to low silica rhyolitic ignimbrites with

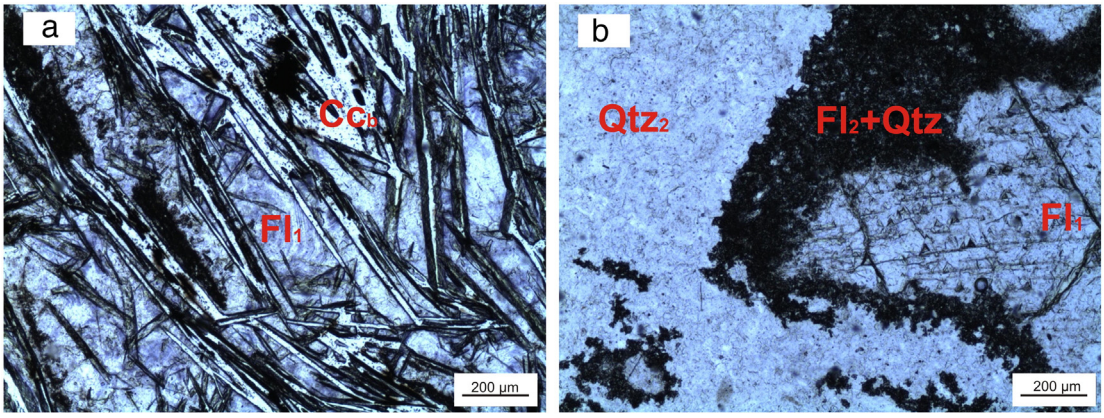

Fig. 2. Photomicrograph of fluorite samples: (a) Coarse fluorite crystals of the first generation (Fl_1) filling the spaces between blade like calcite crystals replaced by chalcedony (Cc_b); (b) first generation fluorite (Fl_1) surrounded by second generation fine fluorite aggregates intergrown with minor quartz (Fl_2 + Qtz) cemented by second silicification stage quartz aggregates (Qtz_2).

geochemical features that indicate an arc tectonic setting with a transpressional structural regime produced by the SRO (Llambías et al., 1993; Kleiman and Japas, 2009). The upper section (264.8 ± 2.3 up to 251.9 ± 2.7 Ma; Rocha-Campos et al., 2011) consists of rhyolitic ignimbrites, andesitic dikes, high silica rhyolitic ignimbrites and lava flows, dacitic to rhyolitic subvolcanics and alkalic basaltic andesites. It has geochemical characteristics transitional between subduction and continental intraplate settings with a transtensional structural regime produced by the PSRO (Llambías et al., 1993; Kleiman and Japas, 2009). Thus, the volcanic character of the CMC shows a transition between a compressive to a progressive extensional tectonic regime that ends with the Triassic rift sedimentary-volcanic successions (Llambías et al., 1993; Kleiman and Salvarredi, 2001).

3. Analytical methods

Mineral samples from four fluorite ore deposit were analyzed for trace and rare earth elements (REE) and Sm–Nd isotopes, and samples from eleven manganese ore deposits were analyzed for metals, trace and rare earth (REE) at Actlabs (Canada) Laboratories. Trace and REE analyses were performed by inductively coupled plasma mass spectrometry technique (ICP-MS).

Rock powder for Sm–Nd analyses was dissolved in a mixture of HF, HNO_3 and $HClO_4$. Before the decomposition the samples were totally spiked with ^{149}Sm-^{146}Nd mixed solution. REEs were separated using conventional cation-exchange techniques. Sm and Nd were separated by extraction chromatography on HDEHP covered Teflon powder. Accuracy of the measurements of Sm and Nd contents is ±0.5% and that of $^{147}Sm/^{144}Nd$ is ±0.5% (2 s). During the analyses the $^{143}Nd/^{144}Nd$ ratios of JNd-1 standard was 0.5121049 ± 0.000019. The analyses were performed on Triton multi-collector mass-spectrometer.

K–Ar analyses in manganese minerals were carried in samples from two ore deposits at the Geochronology Laboratory of the Geological Survey of Chile (SERNAGEOMIN). A previous mineralogical study was made by X-ray diffraction, using a Phillips 1130/90 equipment with Cu anode, 40 kV–20 mA, Ni filter and registration scale of 1000 c per second. Five samples carrying manganese oxides were tested. Only two samples proved to carry K rich minerals with crystallographic characteristics suitable to retain Ar. K analyses were made by atomic absorption spectrometry after chemical attack using Li standards. Isotopic analyses of Ar were made after fusion of two aliquots for each sample using a MS 10S mass spectrometer. The constants used are those proposed by Geochronology Subcommission (Steiger and Jaeger, 1977).

4. Geology of the deposits

4.1. Fluorite deposits

Fluorite ore deposits are mostly hosted by the upper section and very occasionally by the lower section of the CMC. They are regionally distributed but particularly concentrated in the south sector of the SRM, where outcrops of the upper section are more abundant (Fig. 1). Some of these deposits were partially mined between the early 1940s and the early 1980s, with ore grades up to 90% CaF_2 and calculated total reserves of ~480,000 t (Centeno et al., 2009; Mallimacci et al., 2010 and references therein).

The ore bodies are mainly lenticular and minor tabular with length up to 900 m, thickness up to 4 m (but generally not exceeding 0.5 m) and mainly NNW and E–W striking (Centeno et al., 2009; Mallimacci et al., 2010). The deposits consist of one or sometimes two generations of fluorite with colloform, crustiform, cockade and breccia textures and violet, green, white and minor yellow colors. The paragentic sequence begins with lattice bladed calcite (replaced by chalcedony) which is followed by the first generation which consists of coarse crystals of fluorite (Fig. 2a). The second generation is composed by fine fluorite aggregates intergrown with minor quartz (Fig. 2b). Each fluorite generation is followed by a silicification stage that led to quartz aggregates with mosaic, zonal, feathery and comb texture and minor chalcedony. Fluid inclusion studies conducted in fluorite from two different deposits reveal that the mineralizing fluids had low temperature (<110 °C) and salinity (Montenegro, 2013). Scarce pyrite and arsenopyrite are sporadically recognized. Significant base metals geochemical anomalies (particularly in Zn) are occasionally identified (Mallimacci et al., 2010).

In the felsic volcanic host rocks the fluorite veins develop alteration envelopes with a strong pervasive argillic alteration (illite/smectite

Table 1
Sm/Nd isotopic data (in ppm) for fluorite (San Rafael Massif, Argentina). Accuracy of the measurements of Sm and Nd contents is ±0.5%, $^{147}Sm/^{144}Nd$±0.5% (2σ).

Ore deposit	Sample	Sm	Nd	$^{147}Sm/^{144}Nd$	$^{143}Nd/^{144}Nd$	±2σ	ε (Nd_t)
Castaño Viejo	86336	1.585	3.58	0.2679	0.512536	0.000004	−3.85
Tres Alejandros	86322	2.94	9.43	0.1882	0.512438	0.000002	−3.69
Angélica	86102	1.219	2.69	0.2740	0.512503	0.000002	−4.66
Arco Iris	CA11	3.36	5.34	0.3797	0.512694	0.000003	−3.71

εNd values are calculated using an age of 205 Ma. Present day $(^{143}Nd/^{144}Nd)_{CHUR}$ = 0.512683 and $(^{147}Sm/^{144}Nd)_{CHUR}$ = 0.1967. Location of the samples in Table 3.

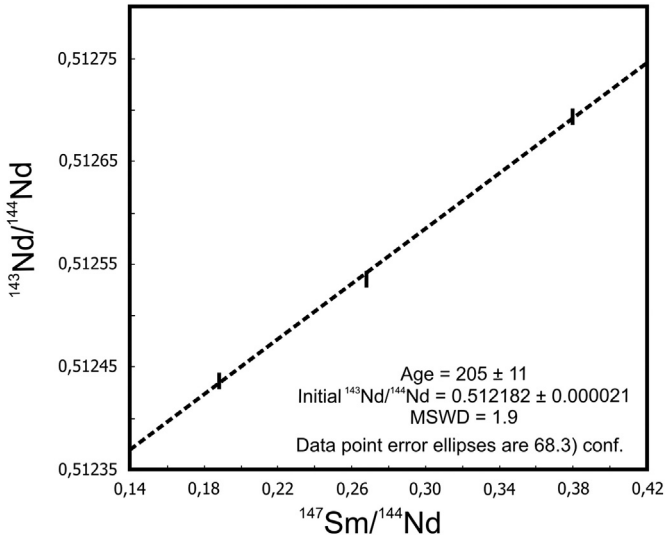

Fig. 3. Sm/Nd isocrone diagram for fluorites from Castaño Viejo, Tres Alejandros and Angélica deposits.

determined by SWIR reflectance spectrometry), a mild pervasive and vein type silicification and minor disseminated pyrite and interstitial fluorite.

4.2. Manganese deposits

Manganese ore deposits are hosted by the upper section of the CMC and particularly occur in the south sector of the SRM. They are concentrated mainly in two mining districts: Santa Cruz and Ethel (Fig. 1). These deposits were partially mined between the 1950s and the 1970s, with ore between 21% and 45% of Mn and calculated total reserves of ~390,000 t (Mallimacci et al., 2010 and references therein).

The ore bodies are tabular and lenticular with length up to 600 m, thickness up to 7 m (but generally not exceeding 0.5 m) and mainly NW, NE and EW striking (Mallimacci et al., 2010).

The deposits consist of different manganese minerals including psilomelane, cryptomelane, hollandite, coronadite, pyrolusite, and minor wad, jacobsite, manganite, groutite, ramsdellite, todorokite, hausmannite and calcofanite with massive, crustiform, colloform and breccia textures (Malvicini and Delpino, 1989). The gangue minerals are iron oxides, calcite, opal, chalcedony and quartz (Mallimacci et al., 2010). Significant geochemical anomalies in Pb, Zn and Mo are frequently identified (c.f. 5.4. below).

In the felsic volcanic host rocks the manganese veins develop alteration envelopes with mild pervasive argillic alteration (illite/smectite determined by SWIR reflectance spectrometry) and silicification with scarce disseminated pyrite and quartz veinlets.

5. Results

5.1. Nd isotopes in fluorite

Four samples of the first generation of fluorite from different deposits hosted by the upper section of the CMC were analyzed for Sm/Nd isotopes. The analytical results are shown in Table 1 and were processed using the ISOPLOT Program (Ludwig, 1999).

Three of the samples, corresponding to violet fluorite, define a linear array in the $^{143}Nd/^{144}Nd$ vs. $^{147}Sm/^{144}Nd$ diagram (Fig. 3), with a low initial $^{143}Nd/^{144}Nd$ (0.512182) which allow establishing an Upper Triassic-Lower Jurassic age (205 ± 11 Ma). The sample from Arco Iris deposit was not considered because it is a yellow fluorite in which Sm and Nd concentrations are high and variable enough to obtain a reliable isochron (Sánchez et al., 2010)

5.2. K/Ar in manganese minerals

Manganese minerals from different ore deposits have been dated, using the K/Ar method, to provide constraints on the age of the mineralization (Table 2). The sample from Dos Marías deposit consisting of pyrolusite, todorokite and ramsdellite of hypogene origin (cf. 5.4. below) returned an age of 71.3 ± 3 Ma. Hypogene cryptomelane (cf. 5.4. below) from Santa Cruz deposit was dated at 16.3 ± 2.4 Ma.

These results allow defining two previously unknown episodes of mineralization, one during the Upper Cretaceous and the other during the Lower Miocene.

5.2.1. Geochemistry of fluorite deposits

Three fluorites that were analyzed for Nd isotopes were also analyzed for trace elements and REE (Table 3).

In general they show low trace element contents, particularly in Sr, Ba, La, Ce and minor in Y with a relatively low total REE content (~30–80 ppm).

The REE chondrite-normalized patterns are very similar for the three samples (Fig. 4). All of them are noticeably enriched in HREE relative to LREE, with slight Ce and strong Eu negative anomalies. Similar results have been recently presented by Coniglio et al. (2014) for other fluorine deposits of the district. The negative Ce anomalies suggest high oxygen fugacities at the source of the hydrothermal fluids and the resultant oxidation of Ce^{+3} and immobilization of Ce^{+4} (Constantopoulos, 1988). However the more negative Eu anomaly of the sample from Arco Iris suggests a lower oxygen fugacity compared with that of the other ore deposits which partially inhibit the conversion of Eu^{+2} to Eu^{+3} (Constantopoulos, 1988).

5.3. Geochemistry of manganese deposits

Chemical analyses of trace elements and REE were performed in manganese oxides from different ore deposits (including those that were dated) in order to establish their origin (Table 3).

The diagram of Fig. 5a shows that the ore samples have a hydrothermal origin, however dubhites (supergene oxides derived from mineralization) also plot in the hydrothermal field. A Pb–Zn plot (Fig. 5b) allows differentiating dubhites (Jorge Alberto deposit and one sample from San Alberto deposit) from other hydrothermal oxides.

Although REE contents are variable for the different samples they display a similar chondrite-normalized diagram in general with a flat pattern and strong negative Eu anomalies (Fig. 6).

Table 2
K/Ar ages for same manganese minerals (San Rafael Massif, Argentina).

Ore deposits	Sample	Mineralogy	% K	Rad. Ar. nl/g	% atm. Ar	Age (2σ)
Dos Marías (Ethel Group)	86303	Pyrolusite, Todorokite Ramsdellite	0.403	1.134	32	71 ± 3
Santa Cruz	86162	Cryptomelane	0.715	0.456	87	16.3 ± 2.4

Location of the samples in Table 3.

Table 3
Trace and REE concentration (ppm) of fluorite and manganese minerals (San Rafael Massif, Argentina).

Ore deposits	Fluorite veins			Manganese veins												
	Arco Iris	Angélica	Castaño Viejo	Santa Cruz	La Negrita	Patricia Mónica	Ingrid	Dos Marías	Dos Marías	Jorge Alberto	San Alberto	San Alberto	Chana	La Jacinta	La Lidia	Lomas Moras
Sample	CA11	86102	86336	86160	86203	86207	86222	86304	86305	86310	86345	86343	86397	86029	86032	86123
Position	35°58′07	36°10′11"	36°01′53"	36°02′38"	35°59′38"	35°59′06"	36°06′26"	36°01′05"	36°01′05"	36°04′04"	36°01′49"	36°01′49"	36°08′22"	35°12′14"	35°46′04"	35°50′19"
	68°30′23″	68°23′43″	68°29′14″	68°27′59″	68°53′09″	68°49′14″	68°27′52″	68°50′18″	68°50′18″	68°27′08″	68°29′29"	68°29′29"	68°23′06″	68°19′51″	68°26′49″	68°47′09″
Cu	–	–	–	<0.5	2.6	66.2	48.4	45.9	<0.5	21.5	20.4	<0.5	14.6	42.3	94.9	105
Mo	–	–	–	365	2	252	184	44	116	1390	10	721	8	55	34	210
Ni	–	–	–	<1	<1	<1	<1	<1	<1	<1	3	3	<1	21	13	38
Pb	–	–	–	320	79	412	45	131	303	1610	86	1580	58	82	644	38
V	–	–	–	200	40	601	103	740	1400	765	68	692	49	44	537	858
Zn	–	–	–	1620	49	485	111	384	679	773	57.1	3240	69.8	303	1150	243
As	–	–	–	243	18.2	98.6	50	49.4	231	133	9.6	684	14.1	2600	891	120
Co	–	–	–	22	43	118	59	28	47	292	9	48	47	28	9	34
Cu	–	–	–	<0.5	2.6	66.2	48.4	45.9	<0.5	21.5	20.4	<0.5	14.6	42.3	94.9	105
Mo	–	–	–	365	2	252	184	44	116	1390	10	721	8	55	34	210
Ni	–	–	–	<1	<1	<1	<1	<1	<1	<1	3	3	<1	21	13	38
Pb	–	–	–	320	79	412	45	131	303	1610	86	1580	58	82	644	38
V	–	–	–	200	40	601	103	740	1400	765	68	692	49	44	537	858
Zn	–	–	–	1620	49	485	111	384	679	773	57.1	3240	69.8	303	1150	243
As	–	–	–	243	18.2	98.6	50	49.4	231	133	9.6	684	14.1	2600	891	120
Co	–	–	–	22	43	118	59	28	47	292	9	48	47	28	9	34
Rb	< 1	< 1	< 1	95	–	113	187	151	80	132	20	36	85	–	–	106
Sr	179	121	100	209	–	<0.5	1100	1400	1890	<0.5	284	348	535	–	–	<0.5
Y	126	51.3	71.1	173	–	56.1	32.4	61.7	71.1	115	150	227	26.6	–	–	44
Cs	< 1	< 1	< 1	12	–	4	57	37	77	19	2	<1	2	–	–	2
Ba	5	6	10	902	–	66276	1110	8360	9270	24335	868	1430	3900	–	–	1940
Zr	16	4	2	–	–	–	–	–	–	–	–	–	–	–	–	–
Nb	12.8	8	6.6	–	–	–	–	–	–	–	–	–	–	–	–	–
La	2.52	2.16	1.63	13.1	–	136	21.4	108	88.1	43.8	22.7	5.67	24.4	–	–	47.2
Ce	4.69	4.41	3.07	33	–	44	40	172	72	104	21	31	50	–	–	33
Pr	1.11	0.63	0.56	–	–	–	–	–	–	–	–	–	–	–	–	–
Eu	0.147	0.281	0.2	0.3	–	2.2	0.4	0.2	0.3	0.7	0.9	1	1.5	–	–	0.8
Nd	5.51	2.62	2.33	26	–	99	32	92	59	64	42	21	107	–	–	79
Sm	3.34	1.13	1.1	4	–	12.8	3.9	17.2	17.5	8.8	5.2	5.5	–	3.4	–	7.4
Eu				–	–	–	–	–	–	–	–	–	–	–	–	–
Tb	2.53	0.79	0.77	2.3	–	2	1.4	3.6	5.8	4.8	2.7	6.7	–	0.9	–	1
Yb	13.2	5.41	5.12	16.1	–	1.6	3.4	4.7	3.3	13.2	7.4	38.4	–	5.5	–	4.2
Gd	7.7	2.19	2.57	–	–	–	–	–	–	–	–	–	–	–	–	–
Dy	19.2	7.4	6.17	–	–	–	–	–	–	–	–	–	–	–	–	–
Ho	4.15	1.84	1.4	–	–	–	–	–	–	–	–	–	–	–	–	–
Er	12.2	5.74	4.47	–	–	–	–	–	–	–	–	–	–	–	–	–
Tm	1.97	0.885	0.731	–	–	–	–	–	–	–	–	–	–	–	–	–
Lu	1.92	0.72	0.831	2.25	–	0.09	0.46	0.64	0.19	1.69	0.87	5.67	–	0.95	–	0.4
Hf	1.3	0.4	0.1	3	–	<1	3	7	1	1	<1	<1	–	3	–	2
Ta	1.7	1.56	1.36	0.7	–	0.6	1.3	0.8	<0.5	2.4	<0.5	<0.5	–	<0.5	–	<0.5
W	2.3	1.7	1.6	83	–	341	155	211	426	282	35	303	–	156	–	137
Th	0.41	0.12	0.08	8.3	–	1.1	12.4	9.7	2.4	19.2	<0.2	0.5	–	4.9	–	8.7
U	0.31	0.09	0.39	10.8	–	11.2	3.3	9.4	10.1	30	2.5	18.2	–	8.3	–	10.1

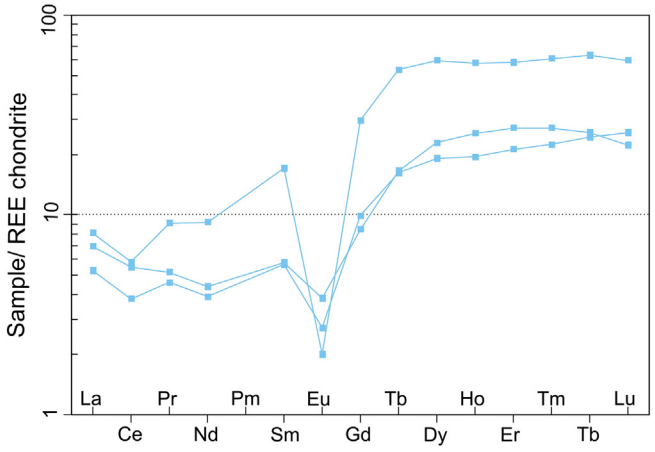

Fig. 4. REE distribution patterns of fluorites. All samples normalized to the chondrite of Boynton (1984).

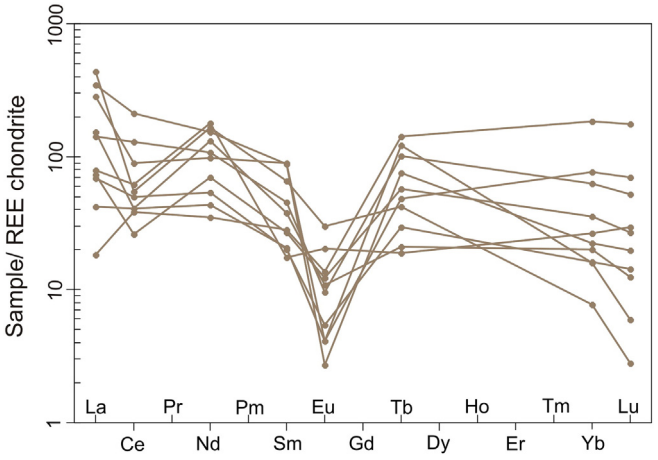

Fig. 6. REE distribution patterns of manganese minerals. All samples normalized to the chondrite of Boynton (1984).

6. Discussion

6.1. Genetic model for SRM F and Mn mineralizations

6.1.1. Fluorite deposits

Fluorine is known to occur in rift-related environments. Climax-type porphyry molybdenum deposits show high F concentrations and are closely related to alkaline rocks in continental rift environments (Ludington and Plumlee, 2009). Alkaline rocks are usually rich in fluorine (e.g. Central Colorado, U.S., Wallace, 2010; Rangel Laccolith, Argentina, Zappettini, 1989). Rift-related deposits are interpreted to be originated by the high heat flow produced during the extension (e.g. the Rio Grande belt, from New Mexico to Colorado, Wallace, 2010). The link between epithermal fluorite veins, usually associated to barite, with rift environments and their characteristics have been summarized by Hora (1996).

During Triassic times the west of Argentina was under an extensional tectonic regime that evolved to different rift systems (Spalletti, 1998). For that time and following the subduction-related and extensional collapse of the CMC a rift basin developed in the SRM. It is represented by the Puesto Viejo Formation which is a syn-rift sequence with interbedded mildly alkaline basalts and andesites and rhyolitic ignimbrites (Spalletti, 1998; Kleiman and Salvarredi, 2001). According to the fossil record this formation has an Anisian age (Bonaparte, 1966) whereas K/Ar whole rock analyses suggest a span age of 251–225 Ma for the ignimbrites and 247–227 Ma for the basaltic rocks (Valencio et al., 1975). A new U/Pb SHRIMP dating of an ignimbrite from this formation returned an age of 235.8 ± 2.0 Ma (Ottone et al., 2013).

The geochemistry of the igneous rocks is consistent with a rift tectonic setting where the mafic rocks have an ocean island basalt (OIB) source and a lower crust contaminant and the ignimbrites come from crustal melts (Kleiman and Salvarredi, 2001). According to the latter authors, this Triassic bimodal magmatism is produced by basaltic underplating in an increasingly extensional tectonic regime coupled with an exceptionally high geothermal gradient due to the preceding subduction and the stationary period of Gondwana, that supplied enough heat to melt a young and warm crust. This geodynamic setting could launch a hydrothermal activity at regional scale producing the abundant fluorite ore deposits of the SRM. This origin is supported by the Sm/Nd isochrone age of 216–194 Ma. Besides, the low initial $^{143}Nd/^{144}Nd$ (0.512182) in the analyzed fluorite suggests an enriched mantle source and thus the involvement of the crust in their genesis (Rollinson, 1993).

6.1.2. Manganese deposits

Mn deposit models in rift-related environments include volcanogenic and detachment-fault-related epithermal deposits. Volcanogenic Mn mineralization is associated to hot spring activity in oceanic environments (Mosier and Page, 1988) or associated to syn-rift and late rift sequences in restricted marine environments (Zappettini et al., 2012).

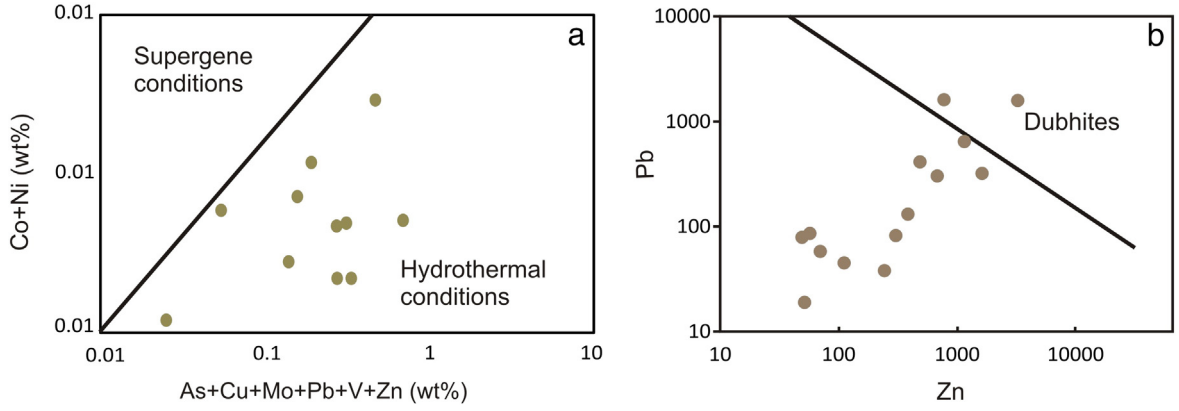

Fig. 5. Diagnostic plot to differentiate supergene and hydrothermal oxides (a) and dubhites from hydrothermal oxides (b) after Nicholson, 1992.

Detachment-fault-related Mn deposits (Long, 2000) consist of rift- and unconformity-related epithermal Mn deposits in continental areas including stratabound accumulations of oxides as well as fracture filling veins associated with normal faulting; both deposits appear to be linked to low-temperature saline alkaline water related or not with basaltic magmatism; original removal of Mn from country rocks would be linked with K metasomatism (Roddy et al., 1988). Such deposits are known worldwide (e.g. in the Middle East, Dill et al., 2013; Arizona, Spencer, 1991; Spain, Crespo and Lunar, 1997).

During the development of the Cretaceous Marianas type subduction zone along the western border of South America, the back arc region was subject to extensional processes. This extensional system was linked to the opening of the Atlantic Ocean and was preceded by the Triassic–Jurassic Gondwanan rifting. Rift related faults resulted in graben and hemigraben systems with faults rooted in the pre-rift successions (Loegering et al., 2013) and the development of rift basins in the continent as well as aulacogenic basins in the continental platform. The latter authors point that seismic information from the Colorado Basin indicates that post-dating the South Atlantic Ocean opening there was a reactivation of the normal faults during the Cretaceous without evidence of structural inversion.

During the Uppper Oligocene–Lower Miocene, at ~19 Ma, an extensional regime affected the region between 35° and 39° S in the Central Andes (Spagnuolo et al., 2012 and references therein). Back-arc extensional geodynamics is in agreement with plate reorganization and a change in the speed and angle of convergence between the Nazca and the South American plates (Kay and Mpodozis, 2002). Evidence of this extensional tectonics is the emplacement of alkaline complexes such as Puesto La Peña Potassic Complex (Zappettini et al., 2013).

The manganese deposits of the SRM have originally been related to the Tertiary magmatism of the region (González Díaz, 1972) as well as to the Pleistocene basalts (García, 1965). Afterwards, they have been linked to the Gondwanan magmatism (Malvicini and Delpino, 1989) and, in particular, to the upper section of the CMC (Carpio et al., 2001). In this latter model, manganese and fluorite deposits have been interpreted jointly with porphyry Mo mineralization as part of a Climax type mineralization (Delpino, 1997; Carpio et al., 2001).

The age obtained for the Dos Marías deposit (71 ± 3 Ma, Upper Cretaceous) allows to discard all previous models. Besides, the obtained age of 16.3 ± 2.4 Ma (Miocene) for the hypogene cryptomelane from Santa Cruz deposit would indicate a second hypogene mineralization episode. The extensional tectonic regime, with the development of rift-related faulting during the Upper Cretaceous and Lower Miocene, is consistent with the generation of two events of Mn mineralizations.

6.2. Source of F and Mn

The source of fluorine has been a matter of debate for explaining the genesis of the main fluorite mining districts around the world. In rift environments, fluorine is a ubiquitous and mobile element usually linked to felsic volcanic rocks related to alkaline magmatism. Van Alstine (1976) has proposed for the Rio Grande Rift related fluorite deposits three possible fluorine sources: volatiles from alkaline magmas, remelting of fluorine-rich alkalic fractions of underlying intrusions and melting of ultramafic mantle rocks bearing fluorine-rich minerals. Seager et al. (1984) have pointed that the age of fluorine veins does not coincide with that of the felsic volcanism but with alkaline mafic rocks.

Geochemical studies conducted by Plumlee et al. (1995) indicate that the presence of fluorine in the mineralizing fluids could only be explained by the addition of HF. On the other hand, Mc Lemore et al. (1998) and Sizaret et al. (2009) have proposed other fluorine sources such as leaching of fluorine and apatite from basement rocks by hot acidic fluids. However Tropper and Manning (2007) have measured the solubility of fluorite in H_2O and H_2O-NaCl at 600-1000 °C and 0.5 to 2.0 GPa, establishing that mineral solubility is low at 600 °C and 0.5 GPa, increasing strongly with rising T and P and with increasing NaCl content in the fluid. Such conditions would point to high P–T igneous and metamorphic environments where F can be mobilized by saline brines.

Chlorine isotopic data from fluorine deposits from the Rio Grande Rift indicate the presence of asthenospheric Cl (Partey, 2004). Considering that Cl and F have a similar chemical behavior during degassing of magmas this author considers a mantle source for fluorine, in coincidence with the model proposed by Plumlee et al. (1995).

In the SRM the upper section of the CMC has a noticeable *a*F evidenced by the presence of accessory topaz and fluorite particularly in the subvolcanic rhyolites (Kleiman and Morello, 2000), indicating increasing F content in the more alkaline rock types. From Eu to Lu the REE pattern of the analyzed fluorites is very similar to that of rocks from the CMC upper section (Fig. 7), but is not typical of a magmatic origin because of the low LREE content (e.g. Hein et al., 1990). Nonetheless, the decoupling in the LREE may be explained as related to the strong argillic alteration of host rocks produced by the hydrothermal activity responsible for the genesis of the fluorite ore deposits because of the potential of the phyllosilicates for LREE adsorption (Alderton et al., 1980). On the other hand, the rocks of the upper section of the CMC were emplaced at surface or at high crust levels, at P–T conditions that preclude F solubilization by saline brines, thus discarding these rocks as the source of F.

The analysis of the available data allows proposing that the mineralizing fluids are not genetically linked to the upper section of the CMC. Considering the solubility and possible sources of F as well as the age of the mineralization, these fluids would have originated during the Triassic rifting when F, assumed to derive from a mantle source, was incorporated as HF related to degassing of a mafic alkaline magma deep-seated in the rift. These mineralizing F-rich fluids would have leached REE from the upper section of the CMC. All the $\varepsilon(Nd_t)$ obtained for the analyzed fluorites (Table 2) are negative and vary between −3.69 and −4.66. Since the REEs are derived from the CMC, the negative $\varepsilon(Nd_t)$ would thus reflect the source of this volcanic unit and not the source of F. The values are consistent with the CMC source, largely derived from crustal melting. It is worth mentioning that a similar model was proposed by Partey (2004) for the Rio Grande Rift fluorite deposits.

The metal contents of the manganese oxides support the hydrothermal origin of the ore deposits that in some cases suffered meteorization. Particularly the samples from Santa Cruz and Dos Marías deposits have a hypogene origin which confirms that there were two mineralization

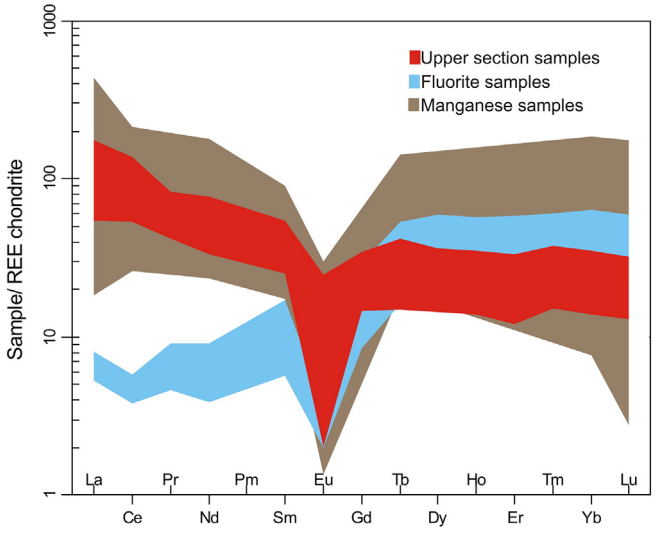

Fig. 7. Comparison between REE distribution patterns of fluorite, manganese minerals and rocks from CMC Upper Section. All samples normalized to the chondrite of Boynton (1984). Geochemical data of the CMC Upper Section (rhyolitic lavas and tuffs) from Kleiman and Japas (2009), Mugas Lobos et al. (2010) and Gómez et al. (in press).

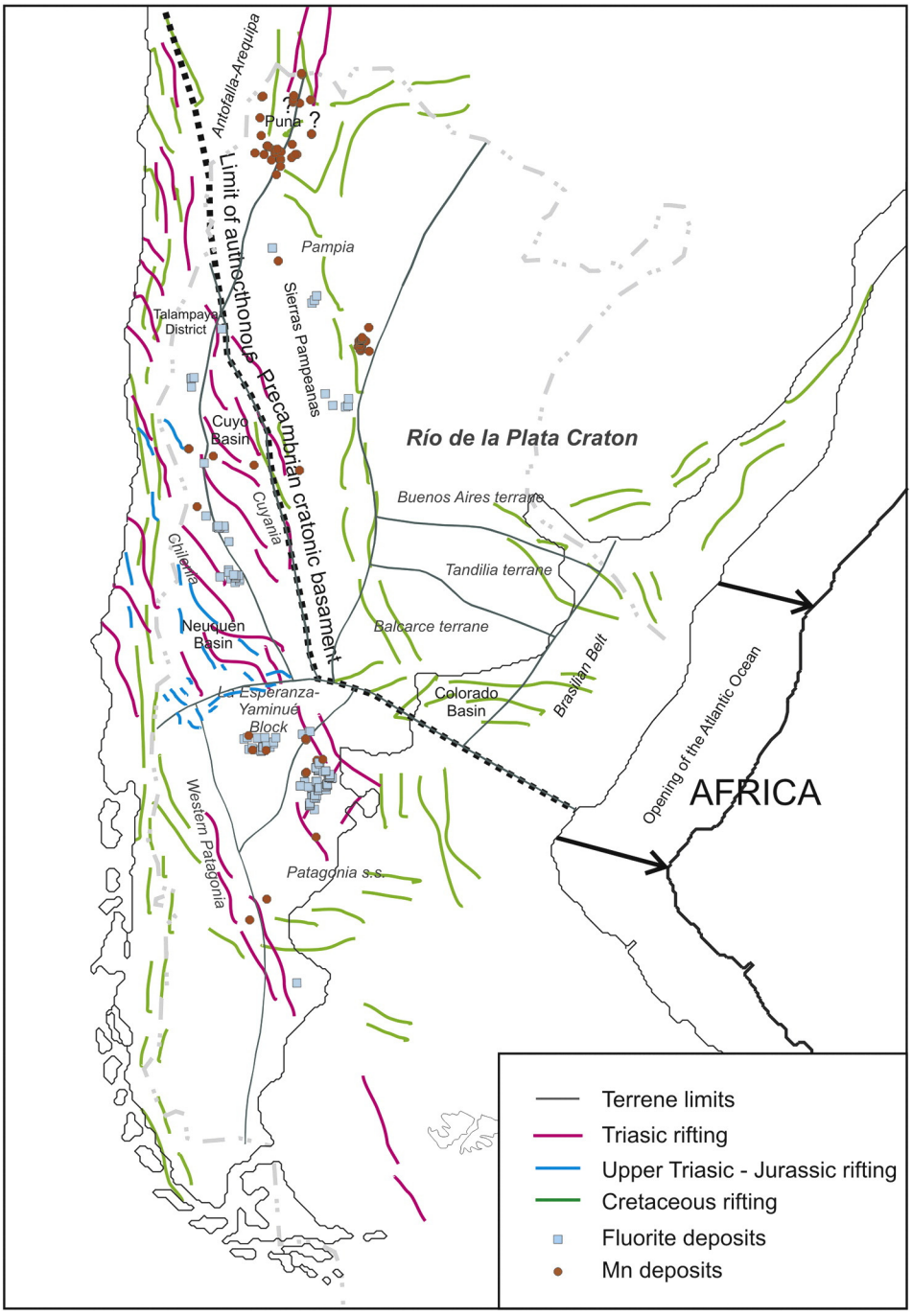

Fig. 8. The Mesozoic rifting in southern South America and related fluorite and manganese mineralizations. Modified from Ramos and Aleman, 2000 and references therein.

episodes. Besides, the geochemical characteristics of the REE suggest a common source for these elements with a pattern roughly similar to that of the CMC upper section which is the host rock of the deposits, suggesting that it provided, through a leaching process, these trace elements.

Since all the manganese minerals of the Mn ore deposits from the SRM contain Mn^{4+} and rhodochrosite is absent, very oxidizing conditions would have prevailed during mineral deposition. Mn is interpreted to have been leached from the upper section volcanics of the CMC as it happens in other similar epithermal Mn districts (e.g. Luis López deposits, Lueth et al., 2004). Mn in igneous rocks occurs in the reduced (2+) state, during its lixiviation from the volcanic units most of the Mn would have been oxidized to 4+. An alternative source of Mn could be the mafic alkaline magmatism of the Triassic rift stage, as suggested for other rift-related Mn deposits (Leal et al., 2008).

6.3. A regional model of rift related mineralizations

The SRM is part of the Gondwanan Orogen that includes an early stage of amalgamation and collision of various terranes against the late Proterozoic margin of Gondwana, a second stage characterized by subduction, Andean-type arc magmatism and subsequent mountain building along the Pacific margin due to cratonward thrusting of the magmatic arc foldbelt, and a third stage of generalized extension during the Pangea break-up that started at Triassic times.

The Triassic extensional phase was mostly confined to a belt parallel to the NNW–SSE oriented Gondwanan margin and its geometry was controlled by the basement fabric (Ramos and Aleman, 2000). The age of the faulting is younger to the south (late Permian in central Argentina to Early Jurassic in Patagonia). The rift basin was filled by red-beds, locally interbedded with bimodal volcanic rocks, with ages that in Argentina are between 240 and 230 Ma (e.g. Cuyo Basin, Spalletti et al., 2008).

The late syn-rift deposits in central Argentina reach the Early Jurassic (Pliensbachian). They are characterized by an extensive bimodal volcanism in isolated and later coalescent rift basins that evolve into the thermal subsidence Neuquén Basin (Franzese and Spalletti, 2001).

During the Late Jurassic and Cretaceous the active rifting persisted with faulting becoming younger from north to south. This extension was active in Bolivia and northern Argentina and is characterized by continental depocenters with associated alkali basalts followed by shallow marine and lacustrine deposits in a thermal SAG setting (Fig. 8). During the Cretaceous the rifting spread to Chile and central Argentina, where it was controlled by old sutures and Triassic faults (Ramos and Aleman, 2000). Finally, there is evidence of an extensional back-arc tectonics during the Lower Miocene.

This extensional tectonic setting that worked from the Triassic to the Lower Miocene was favorable for fluorite and manganese deposits formation. The studied mineralizations in the SRM, controlled by fluid circulation along Triassic, Cretaceous and Lower Miocene faults are good examples of rift-related deposits in a continental environment. Fluorite and manganese deposits formed in similar settings occur in other regions of Argentina (Fig. 8).

Fluorite deposits related to the Triassic faulting occur in La Rioja province (Talampaya district and Chus Chus). The widespread fluorite and minor manganese deposits in northern Patagonia (Aliotta, 1999) are related to the Jurassic extension associated with the opening of the South Atlantic Ocean. In the Sierras Pampeanas epithermal fluorite deposits with ages between 131 ± 22 and 117 ± 26 Ma (Galindo et al., 1996) have been related to Cretaceous extensional events.

Manganese volcanogenic stratabound deposits linked to the syn-rift deposits of the Pre-Cuyano unit (Lower Jurassic) are found in the Neuquén Basin (Zappettini et al., 2012). In the Sierras Pampeanas manganese vein deposits dated at 134.4 ± 0.2 Ma (Brodtkorb and Etcheverry, 2000) are linked to continental rift settings. A normal-fault related manganese deposit of Cenozoic age is known at Ochaqui, Salta province, in the Puna region (Blasco et al., 1996).

7. Conclusions

New isotopic and geochemical data of fluorite and manganese ore deposits of the San Rafael Massif help to establish their genesis and age, as well as to define a regional genetic model.

The fluorite deposits were formed during the Upper Triassic–Lower Jurassic as a result of the Triassic rifting that launched a hydrothermal activity at regional scale with the F probably derived from a mantle source and the REE from the host rocks (upper section of the Choiyoi Magmatic Cycle).

The manganese deposits were formed during two mineralization episodes by hydrothermal fluids that carried Mn from deep sources and leached REE from the upper section of the Choiyoi Magmatic Cycle. One episode was linked to the rift tectonic setting that remained active up to the Upper Cretaceous and the other was related to the back-arc extensional geodynamic setting that worked during the Early Miocene at the SRM latitude.

Both manganese and fluorite deposits formed in extensional tectonic settings within an epithermal environment near the surface, and can be related to the general model of detachment-related deposits. In this scenario, the identification of deeper erosion levels below those represented by the F and Mn veins would help to locate detachment zones that could host Cu–Au mineralization (Long, 2000).

Acknowledgments

We thank Paula Cornejo Peláez for her cooperation during the isotopic analyses of manganese minerals, Eugenia Fonseca who carried out the XRD determinations, Marcelo Yañez who made the spectrometric analyses, César Vásquez who handled the extraction lines at the SERNAGEOMIN and Anabel Gómez who helped with the figures of this paper. We are grateful to Servicio Geológico Minero Argentino (SEGEMAR) for authorizing the publication of this investigation. This research was partially funded by the PIP 11220090100589, CONICET.

References

Alderton, D.H.M., Pearce, J.A., Potts, P.J., 1980. Rare-earth-element mobility during granite alteration: evidence from southwest England. Earth Planet. Sci. Lett. 49, 149–165.
Aliotta, G., 1999. Yacimientos de fluorita de Río Negro y Chubut. In: Zappettini, E.O. (Ed.), Recursos Minerales de la República ArgentinaAnales 35. Instituto de Geología y Recursos Minerales SEGEMAR, pp. 1239–1247.
Blasco, G., Zappettini, E.O., Hong, F., 1996. Hoja Geológica 2566-I, San Antonio de los Cobres: Provincias de Jujuy y Salta, Boletín N° 217. Servicio Geológico Minero Argentino, Buenos Aires.
Bonaparte, J., 1966. Cronología de algunas formaciones triásicas argentinas basadas en restos de tetrápodos. Rev. Asoc. Geol. Argent. 21 (1), 20–38.
Bordonaro, O., Keller, M., Lehnert, O., 1996. El Ordovícico de Ponón-Trehue en la provincia de Mendoza (Argentina): Redefiniciones estratigráficas. Proceedings 13° Congreso Geológico Argentino and 3° Congreso de Exploración de Hidrocarburos, Buenos Aires, Argentina.
Boynton, W.V., 1984. Geochemistry of de rare earth elements: meteorite studies. In: Henderson, P. (Ed.), Rare Earth Element Geochemistry. Elsevier Sciences, Amsterdam, pp. 63–114.
Brodtkorb, M.K., Etcheverry, R., 2000. Edad K/Ar de la mineralización de manganeso de Aguada del Monte, provincia de Córdoba. Rev. Asoc. Geol. Argent. 55 (3), 280–283.
Carpio, F., Mallimacci, H., Rubinstein, N., Salvarredi, J., Sepúlveda, E., Centeno, R., Rosas, M., Vargas, D., 2001. Metalogenia del Bloque de San Rafael, Mendoza. Serie Contribuciones Técnicas, Recursos Minerales 20. Servicio Geológico Minero Argentino, Buenos Aires.
Centeno, R., Rosas, M., Rubinstein, N., 2009. Carta Minero-Metalogenética 3569-IV Embalse El Nihuil, provincia de Mendoza, Boletín N°375. Servicio Geológico Minero Argentino, Buenos Aires.
Cingolani, C.A., Varela, R., 1999. Rb–Sr isotopic age of basement rocks of the San Rafael Block, Mendoza, Argentina. Proceedings 2° South American Symposium on Isotope Geology, Carlos Paz, Argentina.
Coniglio, J., Figueiredo, A.M.G., Brodtkorb, M., D'Eramo, F., Montenegro, T., 2014. Fraccionamiento de elementos tierras raras en fluoritas de yacimientos epitermales del distrito Agua Escondida, Mendoza. Implicancias sobre el origen. Proceedings 19° Congreso Geológico Argentino, Córdoba, Argentina.
Constantopoulos, J., 1988. Fluid inclusions and rare earth element geochemistry of fluorite from South-Central Idaho. Econ. Geol. 83, 626–636.
Crespo, A., Lunar, R., 1997. Terrestrial hot-spring Co-rich Mn mineralization in the Pliocene–Quaternary Calatrava Region (central Spain). In: Nicholson, K., Hein, J.R., Bühn, B., Dasgupta, S. (Eds.), Manganese mineralization: geochemistry and mineralogy of terrestrial and marine deposits. Geological Society Special Publication N° 119, pp. 253–264.
Criado Roque, P., 1972. Bloque de San Rafael. In: Leanza, A. (Ed.), Geología Regional Argentina. Academia Nacional de Ciencias, Córdoba, pp. 283–295.
Delpino, D., 1997. Geología regional y petrología del Complejo Los Corrales paleozoico superior-triásico, provincia de Mendoza. Ph.D. thesis, Universidad Nacional de La Plata, p. 297.
Delpino, D., Pezzutti, N., Godeas, M., Donnari, E., Carullo, M., Núñez, E., 1993. Un cobre porfírico paleozoico superior en el centro volcánico San Pedro, distrito minero el nevado, provincia de Mendoza. Proceedings 12° Congreso Geológico Argentino, Mendoza, Argentina.
Dill, H.G., Pöllmann, H., Techmer, A., 2013. 500 Million years of rift- and unconformity-related Mn mineralization in the Middle East: a geodynamic and sequence stratigraphical approach to the recycling of Mn. Ore Geol. Rev. 53, 112–133.
Espejo, I.S., López Gamundi, O.R., 1994. Source versus depositional controls on sandstone composition on a foreland basin: El Imperial Formation (mid-Carboniferous–lower Permian) San Rafael Basin, western Argentina. J. Sediment. Res. A64, 8–16.
Franzese, J.R., Spalletti, L.A., 2001. Late Triassic–early Jurassic continental extension in southwestern Gondwana: tectonic segmentation and pre-break-up rifting. J. South Am. Earth Sci. 14, 257–270.
Galindo, C., Baldo, E., Pankhurst, R., Casquet, C., Rapela, C., Saavedra, J., 1996. Edad y origen de la fluorita del yacimiento La Nueva (Cabalango, Córdoba, Argentina) en base a geoquímica de isótopos radiogénicos (Nd y Sm). Geogaceta 19, 67–69.
Gargiulo, M., Rubinstein, N., Carpio, F., Salvarredi, J., 2007. Caracterización de la zona de alteración central II, Bloque San Rafael, provincia de Mendoza. Rev. Asoc. Geol. Argent. 62, 387–395.
García, H., 1965. Informe sobre las minas Santa Cruz (manganeso), Liana, Elsiren y Potosí, La Esperanza, Magdalena, Irma y Mirú. Distrito Minero La Escondida, provincia de Mendoza. Servicio Geológico Minero Argentino, Carpeta Nº 1034.
Gómez, A., Rubinstein, N., 2010a. Caracterización genética del distrito minero El Infiernillo, Bloque de San Rafael, provincia de Mendoza. Rev. Asoc. Geol. Argent. 67 (2), 231–238.

Gómez, A., Rubinstein, N., 2010b. Geology of San Pedro Mining District, San Rafael Massif, Argentina. Boll. Geofis. Teor. Appl. 51, 236–239.
Gómez, A., Rubinstein, N., Valencia, V., 2014. Gondwanan magmatism with adakite-like signature linked to Cu (Mo)-porphyry deposits from the San Rafael Massif, Mendoza province, Argentina. Chem. Erde (in press).
González Díaz, E.F., 1972. Descripción Geológica de la Hoja 27 d, San Rafael, Provincia de Mendoza, Boletín N° 132. Servicio Geológico Minero Argentino, Buenos Aires.
Hein, U.F., Lüders, V., Dulski, P., 1990. The fluorite vein mineralzation of the Southern Alpes: combined application of fluid inclusions and rare earth elements (REE) distribution. Mineral. Mag. 54, 325–333.
Hora, Z.D., 1996. Vein Fluorite-barite, in Selected British Columbia Mineral Deposit Profiles. In: Lefebure, D.V., Höy, T. (Eds.), Metallic Deposits vol. 2. British Columbia Ministry of Employment and Investment, pp. 85–88 (Open File 1996-13).
Japas, M.S., Kleiman, L.E., Salvarredi, J.A., 2005. Self-similar behaviour of Triassic rifting in San Rafael, Mendoza, Argentina. Proceedings Gondwana 12°, Mendoza, Argentina.
Kay, S.M., Mpodozis, C., 2002. Magmatism as a probe to the Neogene shallowing of the Nazca plate beneath the modern Chilean flat-slab. J. South Am. Earth Sci. 15, 39–57.
Kleiman, L.E., Japas, M.S., 2009. The Choiyoi volcanic province at 34°S–36°S (San Rafael, Mendoza, Argentina): implications for the late Palaeozoic evolution of the southwestern margin of Gondwana. Tectonophysics 473 (3-4), 283–299.
Kleiman, L.E., Morello, O., 2000. Granates en riolitas y dacitas de la Formación Cerro Carrizalito, Sierra Pintada, Mendoza. Proceedings 5° Reunión de Mineralogía y Metalogenia, La Plata, Argentina.
Kleiman, L.E., Salvarredi, J.A., 2001. Petrología, geoquímica e implicancias tectónicas del volcanismo Triásico (Formación Puesto Viejo), Bloque San Rafael, Mendoza. Rev. Asoc. Geol. Argent. 56, 559–570.
Leal, P.R., Correa, M.J., Ametrano, S.J., Etcheverry, R.O., Brodtkorb, M.K., 2008. The manganese deposits of the Pampean Ranges, Argentina. Can. Mineral. 46, 1215–1233.
Llambías, E.J., Kleiman, L.E., Salvarredi, J.A., 1993. El Magmatismo Gondwánico. Geología Y Recursos Naturales De Mendoza. In: Ramos, V.A. (Ed.), Relatorio 12° Congreso Geológico Argentino y 2° Congreso de Exploración de Hidrocarburos. Mendoza, pp. 53–64.
Loegering, M.J., Anka, Z., Autin, J., di Primio, R., Marchal, D., Rodriguez, J.F., Franke Eduardo Vallejo, D., 2013. Tectonic evolution of the Colorado Basin, offshore Argentina, inferred from seismo-stratigraphy and depositional rates analysis. Tectonophysics 604, 245–263.
Long, K.R., 2000. Preliminary descriptive deposit model for detachment-fault-related mineralization. In: Stoesser, D.B., Heran, W.D. (Eds.), USGS Mineral Deposit Models. USGS Digital Data Series DDS-064.
Ludington, S., Plumlee, G.S., 2009. Climax-type porphyry molybdenum deposits. USGS Open-File Report 2009–1215.
Ludwig, K., 1999. User's Manual for Isoplot/Ex Version 2.06. Special Publication 1. Geochronology Center.
Lueth, V.W., Chamberlin, R.M., Peters, L., 2004. Age of mineralization in the Luis Lopez manganese district, Socorro County, New Mexico, as determined by $_{40}Ar/_{39}Ar$ dating of cryptomelane. New Mexico Bureau of Geology and Mineral Resources, bulletin 160.
Mallimacci, H., Carpio, F., Rubinstein, N., 2010. Carta Minero-Metalogenética 3769-II Agua Escondida, provincias de Mendoza y La Pampa, Boletín N° 375. Servicio Geológico Minero Argentino, Buenos Aires.
Malvicini, L., Delpino, D., 1989. Metalogénesis de los complejos riolíticos de la provincia geológica sanrafaelino pampeana y la comarca norpatagónica, Argentina. Procesos metalogenéticos. Serie Correlación Geológica N°3Universidad Nacional de Tucumán, pp. 63–82.
Mc Lemore, V.T., Giordano, T.H., Lueth, V.W., Witcher, J.C., 1998. Origin of barite–fluorite–galena deposit in the Rio Grande Rift, New Mexico. Guidebook 49. New Mexico Geological Society, pp. 251–264.
Montenegro, T., 2013. Estudio de inclusions fluidas de las fluoritas de Agua Escondida, Mendoza. Proceedings 11° Congreso de Mineralogía y Metalogenia, San Juan, Argentina.
Mosier, D.L., Page, N.J., 1988. Descriptive and Grade–Tonnage models of volcanogenic manganese deposits in oceanic environments—a modification. USGS Bull. 1811, 28.
Mugas Lobos, A.C., Márquez-Zavalía, M.F., Galliski, M.A., 2010. Petrografía y geoquímica de las rocas gondwánicas del proyecto minero Don Sixto, Mendoza. Rev. Asoc. Geol. Argent. 67, 392–402.
Nicholson, K., 1992. Contrasting mineralogical–geochemical signatures of manganese oxides: guides to metallogenesis. Econ. Geol. 87, 1253–1264.
Ottone, E., de la Fuente, M., Monti, M., Naipauer, M., Armstrong, R., Marsicano, C.A., Mancuso, A., 2013. Una edad U/Pb SHRIMP para el Grupo Puesto Viejo y el límite Pérmico–Triásico en el depocentro de San Rafael. Proceedings 6° Simposio Argentino del Paleozoico Superior, Buenos Aires.
Partey, F., 2004. Source of Fluorine and Petrogenesis of the Rio Grande Rift Type Barite–Fluorite–Galena Deposits(MSc. Thesis) Miami University, Miami.
Plumlee, G.S., Goldhaber, M.B., Rowan, E.L., 1995. The potential role of magmatic gases in the genesis of Illinois–Kentucky fluorspar deposits: implications from chemical reaction path modeling. Econ. Geol. 90 (5), 999–1011.
Ramos, V.A., Aleman, A., 2000. Tectonic evolution of the Andes. In: Cordani, U.G., Milani, E.J., Thomaz Filho, A., Campos, D.A. (Eds.), Tectonic Evolution of South America (31st International Geological Congress). Rio de Janeiro, pp. 635–685.
Rocha-Campos, A.C., Basei, M.A., Nutman, A.P., Kleiman, L.E., Varela, R., Llambías, E., Canile, F.M., da Rosa, O.C.R., 2011. 30 Million years of Permian volcanism recorded in the Choiyoi igneous province (W Argentina) and their source for younger ash fall deposits in the Paraná Basin: SHRIMP U–Pb zircon geochronology evidence. Gondwana Res. 19, 509–523.
Roddy, M.S., Reynolds, S.J., Smith, B.M., Ruiz, J., 1988. K-metasomatism and detachment-related mineralization, Harcuvar Mountains, Arizona. Geol. Soc. Am. Bull. 100 (10), 1627–1639.
Rollinson, H.R., 1993. Using Gechemical Data: Evaluation, Presentation. Interpretation, Longman, New York.
Rubinstein, N., Gargiulo, M.F., 2005. Análisis textural de cuarzo hidrotermal del depósito El Pantanito, provincia de Mendoza: nuevos aportes sobre su génesis. Rev. Asoc. Geol. Argent. 60, 96–103.
Rubinstein, N.A., Ostera, H., Mallimacci, H., Carpio, F., 2004. Lead isotopes from gondwanan ore polymetallic vein deposits, San Rafael Massif, Argentina. J. South Am. Earth Sci. 16, 595–602.
Rubinstein, N.A., Gómez, A., Mallimacci, H., 2012. La zona de alteración Arroyo La Chilca–Zanjón del Buitre, bloque de San Rafael, Mendoza. Rev. Asoc. Geol. Argent. 69, 285–293.
Sánchez, V., Cardellach, E., Corbella, M., Vindel, E., Martín-Crespo, T., Boyce, A.J., 2010. Variability in fluid sources in the fluorite deposits from Asturias (N Spain): further evidences from REE, radiogenic (Sr, Sm, Nd) and stable (S, C, O) isotope data. Ore Geol. Rev. 37, 87–100.
Seager, W.R., Shafiqullah, M., Hawley, J.W., Marvin, R.F., 1984. New K–Ar dates from basalts and the evolution of the southern Rio Grande rift. Geol. Soc. Am. Bull. 95, 87–89.
Sepúlveda, E., Bermudez, A., Bordonaro, O., Delpino, D., 2007a. Hoja Geológica 3569-IV, Embalse El Nihuil, provincia de Mendoza, Boletín N° 268. Servicio Geológico Minero Argentino, Buenos Aires.
Sepúlveda, E., Carpio, F., Regairaz, M., Zárate, M., Zanettini, J.C., 2007b. Hoja Geológica 3569-II, San Rafael, provincia de Mendoza, Boletín N° 321. Servicio Geológico Minero Argentino, Buenos Aires.
Sizaret, S., Marcoux, E., Bouce, A., Jebrak, M., Stevenson, R., Ellam, R., 2009. Isotopic (S, Sr, Sm/Nd, D, Pb) evidences for multiple sources in the Early Jurassic Chaillac F-Ba ore deposit (Indre, France). Bull. Soc. Geol. Fr. 180 (2), 83–94.
Spagnuolo, M., Folguera, A., Litvak, V., Rojas Vera, E.A., Ramos, V.A., 2012. Late Cretaceous arc rocks in the Andean retroarc region at 36.5S: evidence supporting a Late Cretaceous slab shallowing. J. South Am. Earth Sci. 38, 44–56.
Spalletti, L.A., 1998. Evolución de las cuencas triásicas del oeste argentino y de la región patagánica. Proceedings 10° Congreso Latinoamericano de Geología and 6° Congreso Nacional de Geología, Buenos Aires, Argentina.
Spalletti, L.A., Fanning, C.M., Rapela, C.W., 2008. Dating the Triassic continental rift in the southern Andes: the Potrerillos Formation, Cuyo Basin, Argentina. Geol. Acta 6 (3), 267–283.
Spencer, J.E., 1991. The Artillery Manganese District in West-Central Arizona. Ariz. Geol. 21 (3), 9–12.
Steiger, R.H., Jaeger, E., 1977. Subcommission on geochronology convention on the use of decay constants in geo- and cosmochronology. Earth Planet. Sci. Lett. 36 (3), 359–362.
Tropper, P., Manning, C.E., 2007. The solubility of fluorite in H_2O and H_2O–NaCl at high pressure and temperature. Chem. Geol. 242, 299–306.
Valencio, D.A., Mendía, J., Vilas, J.F., 1975. Paleomagnetism and K/Ar ages of Triassic igneous rocks from the Ischigualasto–Ischichusca Basin and Puesto Viejo Formation, Argentina. Earth Planet. Sci. Lett. 26 (3), 319–330.
Van Alstine, R.E., 1976. Continental rifts and lineaments associated with Major Fluorspar Districts. Econ. Geol. 71, 977–987.
Wallace, A.R., 2010. Fluorine, fluorite and fluorspar in Central Colorado. USGS Scientific Investigations Report 2010-5113, (61 pp.).
Zappettini, E.O., 1989. Geología y metalogénesis de la región comprendida entre las localidades de Santa Ana y Cobres, provincias de Jujuy y Salta, República Argentina. Universidad de Buenos Aires, (Ph.D. thesis).
Zappettini, E.O., Dalponte, M., Segal, S., Cozzi, G., 2012. Mineralogía y aspectos genéticos del depósito volcanogénico submarino de manganeso "La Casualidad", Cerro Atravesada, Neuquén. Rev. Asoc. Geol. Argent. 69 (4), 544–555.
Zappettini, E.O., Villar, L.M., Hernandez, L., Santos, O., 2013. Geochemical and isotopic constraints on the petrogenesis of the Puesto La Peña undersaturated potassic complex, Mendoza province, Argentina: geodynamic implications. Lithos 162–163, 301–316.